Supporting Information: Three-dimensional stress field around a membrane protein: atomistic and coarse-grained simulation analysis of gramicidin A

[†]Jejoong Yoo, [†,‡]Qiang Cui[1]

[†]*Graduate Program in Biophysics,*
[‡]*Department of Chemistry and Theoretical Chemistry Institute,*
University of Wisconsin, Madison, 1101 University Avenue, Madison, WI 53706

October 28, 2012

[1]Correspondence should be sent to cui@chem.wisc.edu.

1 Additional simulation details

For atomistic simulations the CHARMM force field is used to describe all components of the system: CHARMM22 for proteins (1), CHARMM27r for lipids (2), the original TIP3P (3) for water, and CHARMM ion parameters (4). Parameters for the formyl and ethanolamine groups at the N,C termini are adopted from those for formamide (RESI FORM) and ethanolamine (RESI ETAM) in the CHARMM force field (1). All the atomistic simulations are carried out at constant-temperature and constant-area (NPAT ensemble (5)) using the Gromacs 3.3.3 package (6), which was modified to reproduce CHARMM energy terms accurately. Temperature is maintained constant using the Nosé-Hoover scheme (7, 8). Normal pressure is kept constant at 1 bar using the Parrinello-Rahman scheme (9). A switching scheme from 7 to 10 Å is used for van der Waals interactions. For long-range electrostatic interactions, Particle-Mesh Ewald summation (10) is used with a 14-Å cutoff for the real-space component. SETTLE (11) and LINCS (12) algorithms are used to constrain bonds with hydrogen in water and protein/lipids, respectively. Salt concentration is set to 150 mM by adding appropriate number of sodium and chloride ions. A 2 fs integration time step is used. The dimensions of the DMPC and DSPC systems are approximately $51 \times 51 \times 60$ Å^3 and $52 \times 52 \times 80$ Å^3, respectively.

All CG simulations are carried out under constant temperature and zero surface tension using the Berendsen scheme (13). A 20 fs integration time step is used. Simulation time reported in this study has not been scaled by any factor although a factor of ∼4 has been suggested in the literature (14). Dimensions of the DMPC, DPPC and DSPC systems are approximately $95 \times 95 \times 66$ Å^3, $95 \times 95 \times 74$ Å^3 and $96 \times 96 \times 77$ Å^3.

2 Additional details on stress field calculations

2.1 On the convergence of stress field

Another technical issue worth noting concerns the convergence of the stress calculations, which can be approximately tested by considering the symmetry of the system about the membrane mid-plane. For example, AA stress fields in Fig. 2 of the main text are almost symmetric, thus reasonably converged in ∼200 ns. CG stress fields are converged in 600 ns. Given the rugged energy landscape of AA models, the simulation time for AA models to achieve the same degree of convergence as CG models should be significantly longer (∼ microseconds). Thus, we use AA stress field to only explore the semi-quantitative trends inside and near proteins. For a more complete analysis of membrane deformation energy, we use stress field from CG calculations.

2.2 Decomposition of the stress field

To elucidate the origin of those attractive and repulsive stresses, stress field is decomposed into interaction types in Fig. S1 (AA) and S2 (CG), which helps highlight several features that underlie the mechanical stability of the system. The AA decomposition reveals that contributions by van der Waals (vdW) and bonded interactions are repulsive (positive stress) and attractive (negative stress), respectively (see Fig. S1B,C). By contrast, contributions by AA Coulombic interactions depend on the structural context (Fig. S1A): attractive in the water-lipid interface, attractive along the β-helical axis (or Hydrogen bonds), and repulsive along the peptide bonds. In general, highly repulsive vdW interactions are balanced by highly attractive electrostatic interactions in polar regions (water and water-lipid interface). Structural stability of the protein results from the balance between repulsive vdW and Coulombic interactions and attractive bonded and Coulombic (mainly hydrogen

bonds) interactions. The magnitude of each decomposed stress component can exceed 10,000 bar (see Fig. S1A-D) whereas the magnitudes of the total stress are at most ∼1,000 bar (see Fig. 2 of the main text).

The decomposition of the CG stress profiles by interaction type is shown in Fig. S2A-D. A striking difference between the CG and AA decompositions is that the signs of both vdW and bonded components are flipped in the CG cases. Specifically, contributions by vdW and bonded interactions are attractive and repulsive, respectively, in the CG decompositions. The attractive nature of the vdW interactions in the MARTINI model is reasonable because those vdW interactions are designed to represent the polar interactions as well as the conventional vdW interactions. On the other hand, the CG bonded interactions are repulsive because short-range vdW interactions are merged into the bonded terms during coarse-graining. Nonetheless, total stress profiles in AA and CG simulations are consistent (see Fig. 2 of the main text).

2.3 Contribution of long-range electrostatic components to stress field

Non-bonded interaction setups for the recalculations are identical to those for the production runs except that long-range electrostatic components are omitted (see below) because those non-pairwise interactions are incompatible with Eq. 1 in the main text. This technical problem was circumvented in the previous AA pressure-profile studies (15, 16) by assuming that Ewald components were comparable in lateral and normal directions so that the Ewald components canceled out in the pressure profile, $p_{\mathrm{L}} - p_{\mathrm{N}}$. This assumption is invalid when all components of the stress tensor are of interest as in the present study. Due to this technical difficulty, the reported AA local stress in the present study does not contain the Ewald contribution and contains electrostatic contribution calculated with a cutoff (14 Å) scheme. For example, the contribution to system pressure from Ewald is about −40 bar in the AA DMPC system and −200 bar in the AA DSPC system. Nevertheless, results from AA stress calculations are still meaningful because short-range interactions tend to dictate the shape of local stress field. To explicitly study the dependence of calculated stress field on the cutoff scheme, we carry out stress analysis using a lipid bilayer of 288 DPPC molecules. The simulation and analysis protocols are the same as our simulations for the gA systems. We carry out the production run for 10 ns and perform the subsequent stress analysis using two different cutoff values (14 and 18 Å) for Coulomb interaction; the simulation of 10 ns is clearly not sufficiently long for fully converged pressure profiles but it is appropriate for an analysis of the effect of cutoff. As shown in Fig. S3, change in the cutoff scheme affects stress fields in the lipid head groups, but the overall shapes of stress fields using two different cutoffs are similar. Therefore, for the purpose of this work (comparing AA and CG stress fields), the Coulomb cutoff scheme of 14 Å for the gA systems is appropriate.

2.4 Coupling between lateral and normal stresses

To investigate the coupling between lateral and normal stresses, we plot in Fig. S4 the off-diagonal components of the calculated stress tensors for the CG DPPC system. Clearly, the off-diagonal elements are much smaller than the diagonal ones and therefore can be safely ignored in the discussions in the main text.

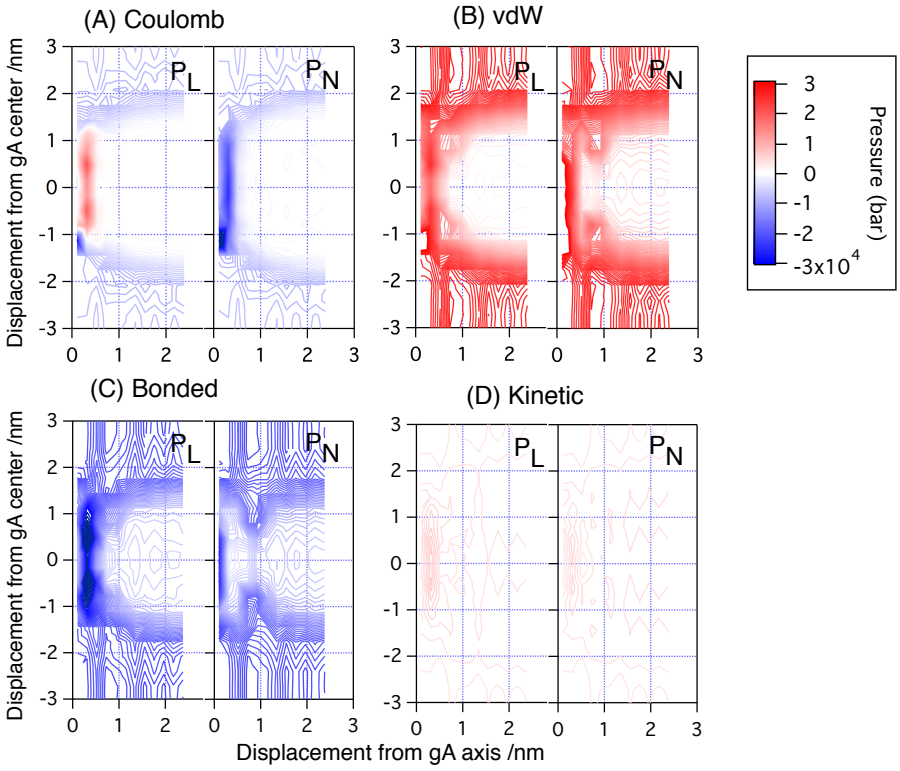

Figure S1: Decomposition of stress field by interaction types in AA DSPC system.

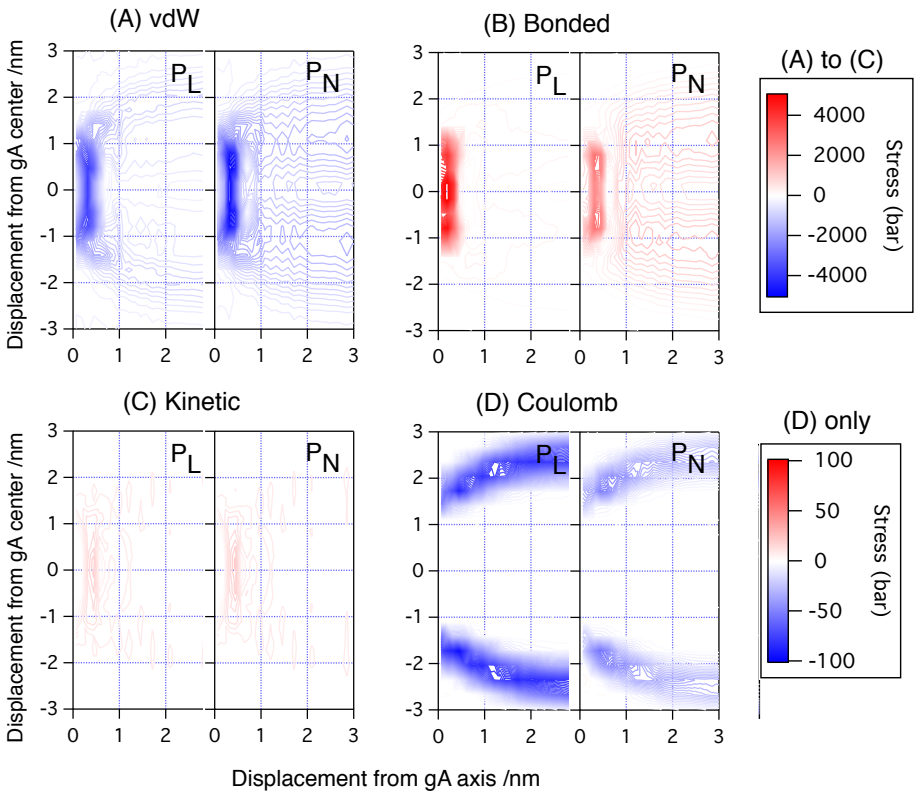

Figure S2: Decomposition of stress field by interaction types in CG DSPC system.

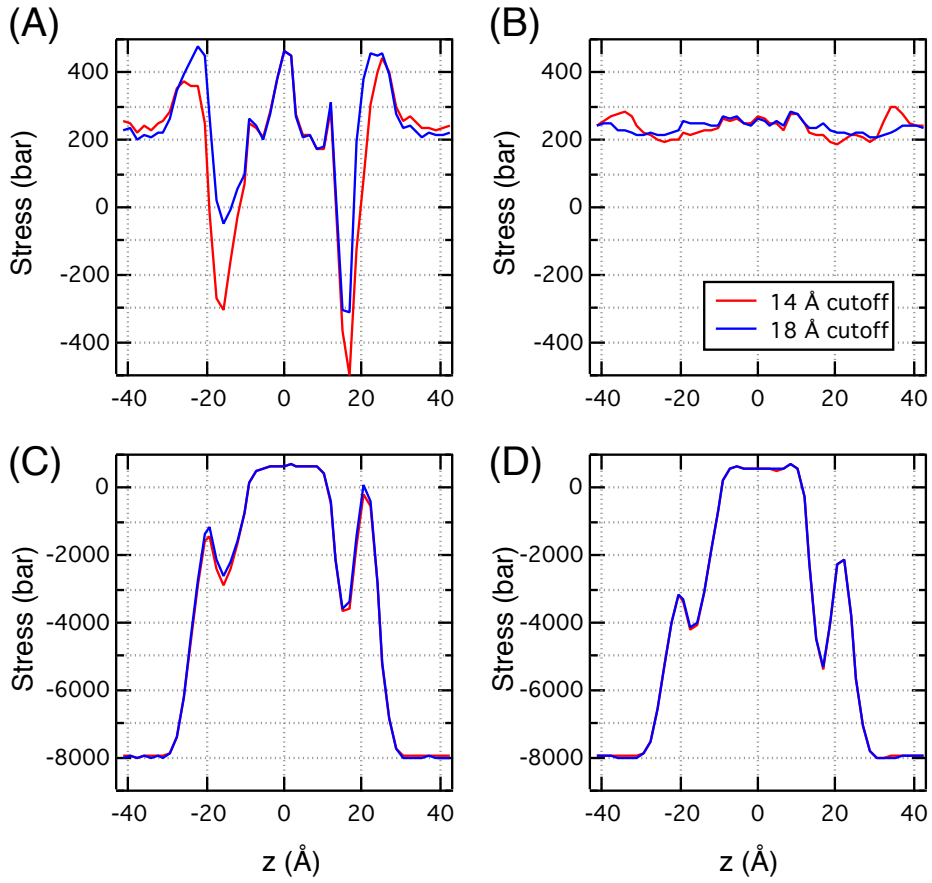

Figure S3: Comparison of stress fields in a pure DPPC bilayer computed using 14- (in red) and 18-Å (in blue) cutoffs from atomistic simulations. Lateral and normal total stresses are shown in (A) and (B), respectively. Nonbonded Coulombic contributions to lateral and normal stresses are shown in (C) and (D), respectively.

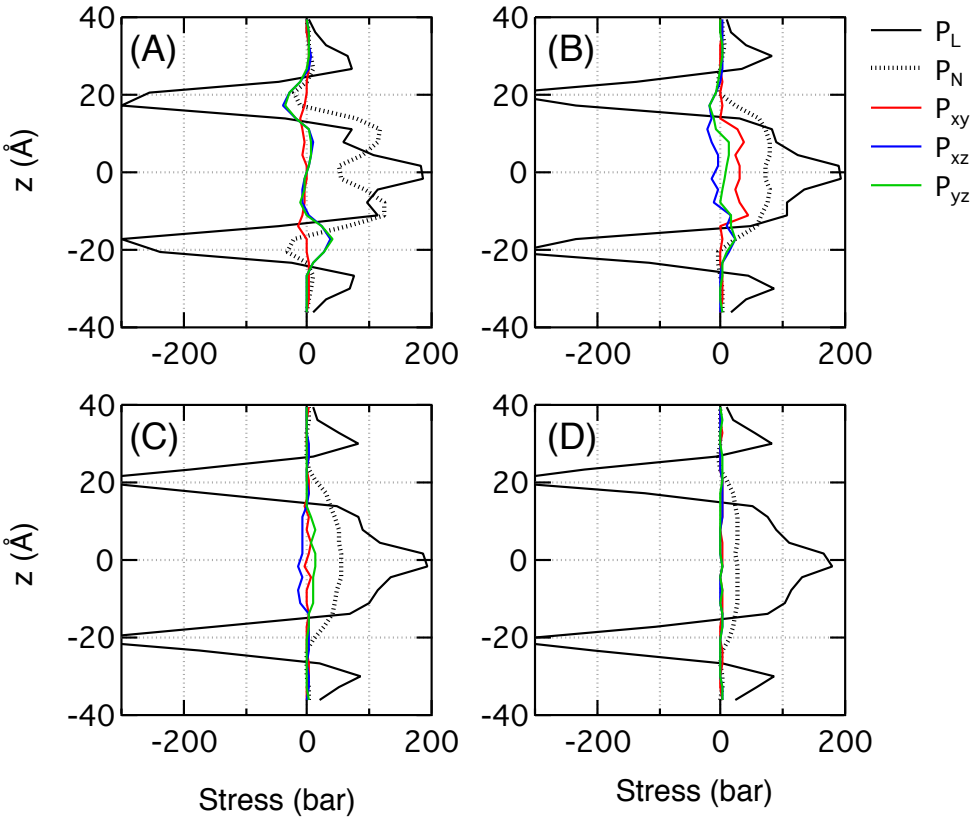

Figure S4: Stress tensor components in the CG DPPC system are shown as a function of normal displacement from the gA dimer in four regions: $10 < r < 15$ Å (A), $15 < r < 20$ Å (B), $20 < r < 25$ Å (C), and $25 < r < 30$ Å (D). Off-diagonal components p_{xy}, p_{xz}, and p_{yz} are shown in red, blue, and green lines, respectively. For comparison, p_L and p_N are also shown in black solid and dotted lines, respectively. Note that the off-diagnonal components are significantly smaller than p_L and p_N.

References

1. MacKerell, A. D. J., D. Bashford, M. Bellott, R. L. Jr.Dunbrack, J. D. Evenseck, M. J. Field, S. Fischer, J. Gao, H. Guo, S. Ha, D. Joseph-McCarthy, L. Kuchnir, K. Kuczera, F. T. K. Lau, C. Mattos, S. Michnick, T. Ngo, D. T. Nguyen, B. Prodhom, W. E. I. Reiher, B. Roux, M. Schlenkrich, J. C. Smith, R. Stote, J. Straub, M. Watanabe, J. Wiórkiewicz-Kuczera, D. Yin, and M. Karplus, 1998. All-atom empirical potential for molecular modeling and dynamics studies of proteins. *J. Phys. Chem. B* 102:3586–3616.

2. Feller, S. E., and A. D. MacKerell Jr., 2000. An improved empirical potential energy function for molecular simulations of phospholipids. *J. Phys. Chem. B* 104:7510–7515.

3. Jorgensen, W. L., J. Chandrasekhar, J. D. Madura, R. W. Impey, and M. L. Klein, 1983. Comparison of simple potential functions for simulating liquid water. *J. Chem. Phys.* 79:926–935.

4. Beglov, D., and B. Roux, 1994. Finite representation of an infinite bulk system: Solvent boundary potential for computer simulations. *J. Chem. Phys.* 100:9050–9063.

5. Feller, S. E., Y. H. Zhang, R. W. Pastor, and B. R. Brooks, 1995. Constant-pressure molecular-dynamics simulation - the Langevin piston method. *J. Chem. Phys.* 103:4613–4621.

6. Van Der Spoel, D., E. Lindahl, B. Hess, G. Groenhof, A. E. Mark, and H. J. C. Berendsen, 2005. GROMACS: fast, flexible, and free. *J. Comput. Chem.* 26:1701–18.

7. Nose, S., and M. L. Klein, 1983. Constant pressure molecular dynamics for molecular systems. *Mol. Phys.* 50:1055–76.

8. Hoover, W. G., 1985. Canonical dynamics: Equilibrium phase-space distributions. *Phys. Rev. A* 31:1695–.

9. Parrinello, M., and A. Rahman, 1981. Polymorphic transitions in single crystals: A new molecular dynamics method. *J. Appl. Phys.* 52:7182–90.

10. Darden, T., D. York, and L. Pedersen, 1993. Particle mesh Ewald: An N log(N) method for Ewald sums in large systems. *J. Chem. Phys.* 98:10089–92.

11. Miyamoto, S., and P. A. Kollman, 1992. SETTLE: An analytical version of the SHAKE and RATTLE algorithms for rigid water models. *J. Comput. Chem.* 13:952–62.

12. Hess, B., H. Bekker, H. J. C. Berendsen, and J. G. E. M. Fraaije, 1997. LINCS: A linear constraint solver for molecular simulations. *J. Comput. Chem.* 18:1463–72.

13. Berendsen, H. J. C., J. P. M. Postma, W. F. Van Gunsteren, A. Dinola, and J. R. Haak, 1984. Molecular dynamics with coupling to an external bath. *J. Chem. Phys.* 81:3684–3690.

14. Marrink, S. J., H. J. Risselada, S. Yefimov, D. P. Tieleman, and A. H. de Vries, 2007. The MARTINI force field: coarse grained model for biomolecular simulations. *J. Phys. Chem. B* 111:7812–7824.

15. Lindahl, E., and O. Edholm, 2000. Spatial and energetic-entropic decomposition of surface tension in lipid bilayers from molecular dynamics simulations. *J. Chem. Phys.* 113:3882–3893.

16. Gullingsrud, J., and K. Schulten, 2004. Lipid bilayer pressure profiles and mechanosensitive channel gating. *Biophys. J.* 86:3496–509.